

Reactions of liquid and solid aluminum clusters with N₂: The role of structure and phase in Al₁₁₄ +, Al₁₁₅ +, and Al₁₁₇ +

Baopeng Cao, Anne K. Starace, Oscar H. Judd, Indrani Bhattacharyya, and Martin F. Jarrold

Citation: *The Journal of Chemical Physics* **141**, 204304 (2014); doi: 10.1063/1.4901895

View online: <http://dx.doi.org/10.1063/1.4901895>

View Table of Contents: <http://scitation.aip.org/content/aip/journal/jcp/141/20?ver=pdfcov>

Published by the [AIP Publishing](#)

Articles you may be interested in

[Reaction of aluminum clusters with water](#)

J. Chem. Phys. **134**, 244702 (2011); 10.1063/1.3602326

[Metal clusters with hidden ground states: Melting and structural transitions in Al₁₁₅ +, Al₁₁₆ +, and Al₁₁₇ +](#)

J. Chem. Phys. **131**, 124305 (2009); 10.1063/1.3224124

[The chemistry of nitrogen oxides on small size-selected cobalt clusters, Co_n +](#)

J. Chem. Phys. **130**, 064305 (2009); 10.1063/1.3075583

[Guided ion beam studies of the reaction of Ni_n + \(n=2–16\) with D₂: Nickel cluster-deuteride bond energies](#)

J. Chem. Phys. **117**, 132 (2002); 10.1063/1.1481855

[Effects of pressure and temperature on the reactions of niobium cluster cations with hydrogen and deuterium](#)

J. Chem. Phys. **115**, 3629 (2001); 10.1063/1.1389302



Reactions of liquid and solid aluminum clusters with N₂: The role of structure and phase in Al₁₁₄⁺, Al₁₁₅⁺, and Al₁₁₇⁺

Baopeng Cao, Anne K. Starace, Oscar H. Judd, Indrani Bhattacharyya,
and Martin F. Jarrold^{a)}

Chemistry Department, Indiana University, 800 East Kirkwood Avenue, Bloomington, Indiana 47401, USA

(Received 25 September 2014; accepted 3 November 2014; published online 24 November 2014)

Kinetic energy thresholds have been measured for the chemisorption of N₂ onto Al₁₁₄⁺, Al₁₁₅⁺, and Al₁₁₇⁺ as a function of the cluster's initial temperature, from around 200 K up to around 900 K. For all three clusters there is a sharp drop in the kinetic energy threshold of 0.5–0.6 eV at around 450 K, that is correlated with the structural transition identified in heat capacity measurements. The decrease in the thresholds corresponds to an increase in the reaction rate constant, $k(T)$ at 450 K, of around 10⁶-fold. No significant change in the thresholds occurs when the clusters melt at around 600 K. This contrasts with behavior previously reported for smaller clusters where a substantial drop in the kinetic energy thresholds is correlated with the melting transition. © 2014 AIP Publishing LLC. [<http://dx.doi.org/10.1063/1.4901895>]

INTRODUCTION

There have recently been a number of studies of the melting of size-selected metal clusters.^{1–6} Unlike macroscopic crystals which melt at a single temperature, metal clusters melt over a range of temperatures where liquid-like and solid-like clusters coexist in a dynamic equilibrium.^{7–9} There are large fluctuations in the melting temperatures as a function of cluster size and considerable effort has been invested into identifying the cause of these fluctuations.^{10–13}

In this paper we investigate how the chemical reactivity changes when the clusters melt. There have been a number of studies of metal cluster reactivity in the past, but these studies have mainly focused on the size-dependent variations in the reaction rates.^{14–24} The studies reported here have more in common with surface reactive scattering studies, where a reagent beam impinges on a well-characterized surface.^{25–27} In our studies we are able to vary the collision energy and the temperature of the cluster surface over wide ranges, investigating reactions on both the solid-like and liquid-like phases of the cluster. Not much is known about the reactivity of liquid metal surfaces because most metals melt at such a high temperature that the chemistry is limited and measurements are difficult. However, metal clusters generally have depressed melting temperatures, and because of the large size-dependent fluctuations, it is reasonable to expect that some cluster sizes will have melting temperatures that are relatively low, perhaps even close to room temperature. Thus the study of the reactions on liquid and solid metal clusters is expected to reveal new chemistry.

We recently reported studies of the reactions of Al₄₄^{+/-} and Al₁₀₀⁺ with N₂.^{28,29} N₂ chemisorbs onto these aluminum clusters, however, there is a substantial kinetic energy threshold that must be overcome for chemisorption to occur. The kinetic energy thresholds were measured using an ion beam

technique, where a beam of clusters ions is passed through a gas cell containing N₂, and the cross section for product formation is determined as a function of the ions relative kinetic energy with the N₂. The kinetic energy thresholds were determined as a function of the cluster's initial temperature over a wide temperature range that covered both the solid-like and liquid-like states. For both Al₄₄^{+/-} and Al₁₀₀⁺, a substantial drop in the kinetic energy threshold for N₂ chemisorption occurs when the clusters melt. The kinetic energy threshold is around 1 eV lower with the liquid-like clusters than with the solid-like.

Melting temperatures have been measured for aluminum clusters using an approach where the heat capacity is determined as a function of the temperature.³⁰ The signature of the melting transition is a peak in the heat capacity due to the latent heat, and most clusters (including Al₄₄^{+/-} and Al₁₀₀⁺) show a single, well-defined peak.^{31–38} Cationic clusters with 115, 116, and 117 atoms, on the other hand, show two clearly resolved peaks.³⁹ In these cases, the lower temperature peak was attributed to a structural transition and the higher temperature peak to the melting transition. In this paper we present kinetic energy thresholds measured for the chemisorption of N₂ onto Al₁₁₄⁺, Al₁₁₅⁺, and Al₁₁₇⁺, as a function of temperature (we did not perform threshold measurements for Al₁₁₆⁺). The behavior reported here differs from that found with the smaller clusters (Al₄₄^{+/-} and Al₁₀₀⁺) where a substantial drop in the kinetic energy threshold for N₂ chemisorption occurs when the clusters melt.

EXPERIMENTAL METHODS

The apparatus used to study reactions between aluminum clusters and N₂ has been described in detail in Refs. 29 and 30. The aluminum clusters are generated by pulsed laser vaporization of a liquid aluminum target in a continuous flow of helium buffer gas.⁴⁰ After formation, the clusters are carried through a 10 cm long temperature variable extension where

^{a)} Author to whom correspondence should be addressed. Electronic mail: mjf@indiana.edu

their temperature is set by equilibration with the walls of the extension through collisions with the helium buffer gas. The temperature of the extension is regulated to better than ± 2 K by a programmable temperature/process controller.³⁰ The cluster ions that exit the temperature-variable extension are focused into a quadrupole mass spectrometer set to transmit a single cluster size. For the studies described here, the size-selected clusters are focused into an ion beam and directed through a low pressure reaction cell containing nitrogen gas. The pressure of the nitrogen was kept sufficiently low that the clusters experience, on average, around one collision as they travel through the reaction cell. Measurements performed as a function of pressure showed that the total product abundance scaled linearly with the pressure, so multiple collisions do not significantly affect the results. The product ions and unreacted cluster ions that exit the reaction cell are focused into a second quadrupole mass spectrometer where they are analyzed and then detected by an off-axis collision dynode (10 kV) and dual microchannel plates.

EXPERIMENTAL RESULTS

The main product observed from the reactions of Al_{114}^+ , Al_{115}^+ , and Al_{117}^+ with N_2 results from the addition of N_2 to yield Al_nN_2^+ . As discussed below, this product has a kinetic energy threshold. This observation, along with the fact that the Al_nN_2^+ product is observed over a wide range of cluster temperatures and relative kinetic energies, indicates that the N_2 is chemisorbed onto the aluminum clusters. A weakly bound physisorbed N_2 should rapidly desorb at high cluster temperatures.

In addition to the Al_nN_2^+ product, some secondary products are observed at high relative kinetic energies and high cluster temperatures. The main secondary product ions are $\text{Al}_{n-2}\text{N}_2^+/\text{Al}_{n-1}^+$ (which differ in mass by 1 Da and were not resolved in the product ion mass spectrum), $\text{Al}_{n-3}\text{N}_2^+/\text{Al}_{n-2}^+$, and $\text{Al}_{n-3}\text{N}^+$. These products are similar to those observed in the reactions of $\text{Al}_{44}^{+/-}$ with N_2 .²⁹ For $\text{Al}_{44}^{+/-}$ the secondary products are dominant at high cluster temperatures, in contrast, for Al_{114}^+ , Al_{115}^+ , and Al_{117}^+ the secondary products never amount to more than a few percent of the Al_nN_2^+ product. For the $\text{Al}_{n-3}\text{N}^+$ product mentioned above, the corresponding neutral product is probably Al_3N (Al_3N is known to be a stable aluminum/nitrogen cluster^{41,42}). The observation of this product indicates that the aluminum clusters can cleave the N_2 bond.

As noted above, the dominant product observed from the reactions of Al_{114}^+ , Al_{115}^+ , and Al_{117}^+ with N_2 results from the addition of N_2 to yield Al_nN_2^+ . The reaction cross sections for N_2 addition were obtained from

$$\sigma = \left(\frac{I_{\text{Al}_n\text{N}_2}}{I_{\text{Al}_n\text{N}_2} + \sum I_p} \right) \times \ln \left[\frac{I_{\text{Al}_n} + I_{\text{Al}_n\text{N}_2} + \sum I_p}{I_{\text{Al}_n}} \right] \frac{1}{Nl}, \quad (1)$$

where $I_{\text{Al}_n\text{N}_2}$ is the intensity of the Al_nN_2^+ addition product ions in the measured mass spectrum, I_p are the intensities of the other product ions, and I_{Al_n} is intensity of the remaining, unreacted cluster ions, N is the neutral reagent number density, and l is the length of the reaction cell. The measured

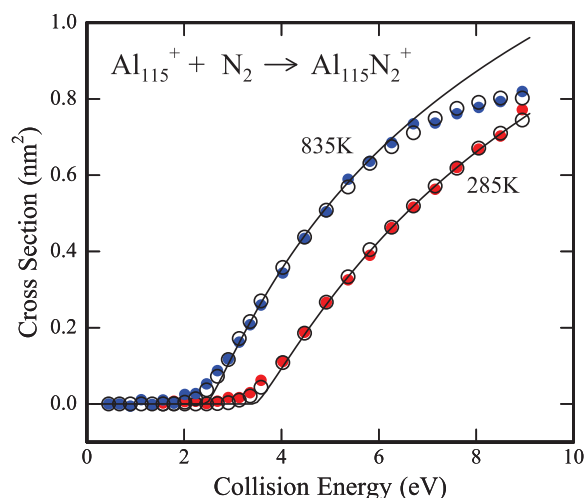


FIG. 1. Cross sections measured for formation of $\text{Al}_{115}\text{N}_2^+$ from collisions of Al_{115}^+ with N_2 . The cross sections are plotted as a function of relative kinetic energy for initial cluster temperatures of 285 K (red points) and 835 K (blue points). The unfilled circles are fits to the measured cross sections with the model described in the text. The solid line shows the empirical cross section function (the part of Eq. (2) before the integral) that provides the best fit to the measured cross sections.

cross sections for N_2 addition to Al_{115}^+ are shown in Figure 1 plotted against relative kinetic energy. Results are shown for two cluster temperatures: 285 K (red points) and 835 K (blue points). As noted above, the cross sections show a kinetic energy threshold and the threshold at 835 K is over 1 eV lower than the threshold at 285 K. We performed similar measurements for a range of temperatures between 185 K and 885 K for all three clusters. The results for Al_{114}^+ and Al_{117}^+ are similar to those shown in Figure 1 for Al_{115}^+ .

ANALYSIS OF EXPERIMENTAL RESULTS

To determine accurate values for the kinetic energy thresholds it is necessary to account for the experimental factors which cause the threshold to broaden and shift. For a reaction driven solely by kinetic energy, the two contributors are the kinetic energy distribution of the ion beam and the thermal motion of the target gas. For the reactions studied here, the mass of the ion is much greater than the mass of the target and the contribution from the spread in the ion beam energy can be safely neglected. So to determine the true kinetic energy threshold, the measured cross sections are fit with an assumed function which is broadened to account for the thermal motion of the target gas molecules. The function used here is

$$\sigma(E) = \sigma_0 \frac{(E - E_0)^n}{E} \int dE_T P(E_T) e^{-k\{E_T + E + D(\text{N}_2), D(\text{Al})\}t}. \quad (2)$$

The part of this equation before the integral is the widely used empirical cross section function where σ_0 is the cross section scaling factor, E is the relative kinetic energy, E_0 is the kinetic energy threshold of the reaction, and n is an adjustable parameter.⁴³ With $n = 1$ the cross section function is the simple line of centers model.⁴⁴ Note that the cross section function does not incorporate any dependence on the internal energy.

The integral in Eq. (2) accounts for the dissociation of the Al_nN_2^+ product when it is highly excited (i.e., at high cluster temperatures and high relative kinetic energies). Dissociation of Al_nN_2^+ leads to the formation of secondary products and causes the cross sections for the Al_nN_2^+ product to roll over.^{45–50} This rollover is not immediately apparent in the measured cross sections shown in Figure 1; however, it is much more important for smaller clusters.²⁹ We assume that the lowest energy dissociation pathway is loss of an aluminum atom from the Al_nN_2^+ product. The dissociation energy for this process is similar to the dissociation energy of an Al atom from the Al_n^+ cluster. Loss of N_2 from Al_nN_2^+ is expected to be competitive with loss of an Al atom and may be lower in energy.²⁹ However, the choice of the lowest energy dissociation pathway is not important because there is not very much product dissociation for the cluster sizes examined here. $k\{E_T + E + D(\text{N}_2), D(\text{Al})\}$ in Eq. (2) is the rate constant for dissociation of the Al_nN_2^+ product to give $\text{Al}_{n-1}\text{N}_2^+ + \text{Al}$. $E_T + E + D(\text{N}_2)$ is the total internal energy of the Al_nN_2^+ product, and $D(\text{Al})$ is the dissociation energy for loss of an Al atom. $D(\text{N}_2)$ is the dissociation energy of Al_nN_2^+ to yield Al_n^+ and N_2 , and E_T is the internal energy of the cluster before its collision with an N_2 molecule. $P(E_T)$ in Eq. (2) is the probability that the ion has an internal energy E_T . $P(E_T)$ is related to the initial temperature of the cluster which is set by the temperature of the temperature-variable extension; it is calculated by statistical thermodynamics using the vibrational frequency distribution generated by a modified Debye model.⁵¹ The rate constants were estimated using the quantum RRR model.⁵² Note that the rate constant depends on both $D(\text{Al})$ and $D(\text{N}_2)$.

To fit the assumed cross section function to the measured cross sections it must be averaged over the distribution of collision energies that result from the thermal motion of the target gas. This is achieved by averaging over 10^3 vectors where the direction is randomly selected and the speed is randomly selected from a Maxwell-Boltzmann velocity distribution. In the threshold region, the velocity of the cluster ion is much larger than the velocity of the N_2 . There are five variables in Eq. (2) that can be adjusted to fit to the measured cross sections. σ_0 , E_0 , $D(\text{Al})$, and $D(\text{N}_2)$ were adjusted automatically using a least squares procedure while n was adjusted manually. The value of n was varied in increments of 0.25 starting at 0.75 and going up to 1.75. In about half the cases $n = 1.25$ provided the best fit (lowest standard deviation) and in the other half $n = 1.50$ provided a slightly better fit. The fits degrade quickly as n moves away from 1.25 and 1.50. Since the results did not provide a strong statement about the best value for n , in what follows we report averages of the $n = 1.25$ and 1.50 values for the kinetic energy thresholds (E_0).

The open points in Figure 1 show the fits of the model (with $n = 1.25$) to the measured cross sections for Al_{115}^+ at 285 K and 885 K. The solid line shows the empirical cross section function (the part of Eq. (2) before the integral) that provides the best fit to the measured cross sections. The significant deviation between the empirical cross section function and the points that occurs at high relative kinetic energies for an initial cluster temperature of 835 K results from dissociation of the $\text{Al}_{115}\text{N}_2^+$ product.

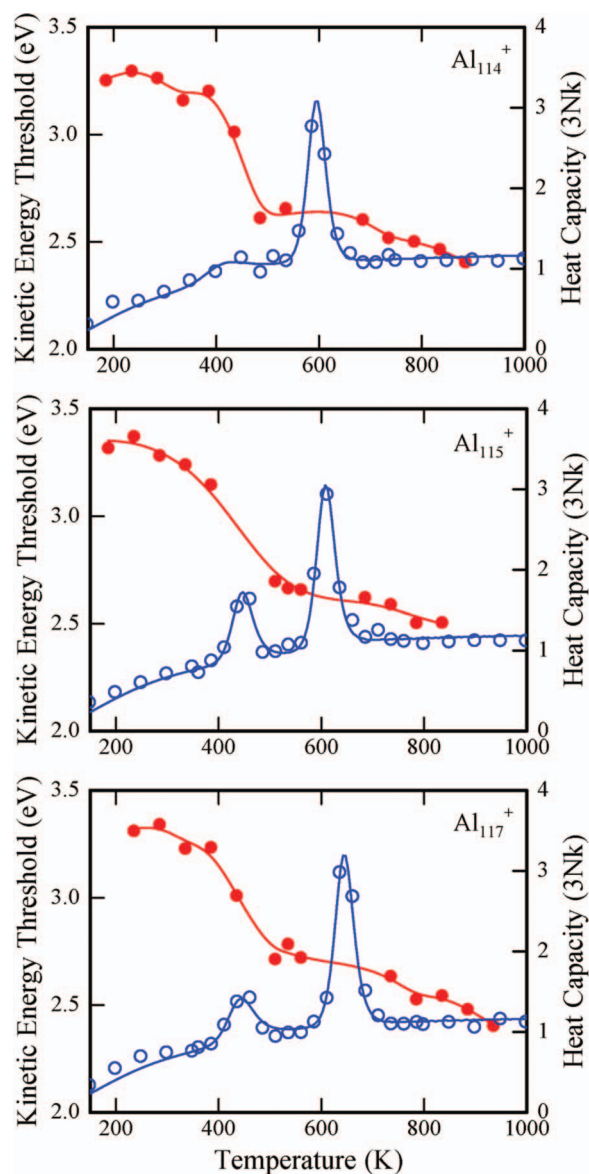


FIG. 2. The red points show kinetic energy thresholds for chemisorption of N_2 onto Al_{114}^+ , Al_{115}^+ and Al_{117}^+ (left scale) plotted as a function of temperature. The blue points show the heat capacities measured as a function of temperature (right scale). The heat capacities are in units of the classical value $3Nk_B$ with $N = 3n - 6 + 3/2$ (n is the number of atoms). The estimated relative uncertainty in the threshold values is ± 0.1 eV. The uncertainty in the temperature scale is ± 2 K. The red and blue lines are guides.

Kinetic energy thresholds deduced from the fits for the reactions of Al_{114}^+ , Al_{115}^+ and Al_{117}^+ with N_2 are presented in Figure 2 where they are plotted as the red points against the initial cluster temperature. In these measurements, we avoided temperatures where the internal energy of the clusters had the potential to undergo large changes with a small change in conditions (i.e., at the peaks in the heat capacities). The points shown in Figure 2 are an average of 2–3 independent measurements. The estimated relative uncertainty in the average threshold values is ± 0.1 eV. The uncertainty in the temperature scale is ± 2 K. The results for all three clusters are similar. At room temperature the reaction thresholds are around 3.2–3.3 eV. As the temperature is raised the thresholds decrease gradually and then there is a sharp drop for

initial cluster temperatures of 400–500 K to around 2.6–2.7 eV, and then the thresholds gradually decrease further reaching around 2.5–2.6 eV at 800 K.

DISCUSSION

As noted above, the persistence of the Al_nN_2^+ products over a wide range of cluster temperatures indicates that the N_2 must be chemisorbed, and the observation of $\text{Al}_{n-3}\text{N}^+$ as secondary products indicates that at least some of the N_2 is dissociatively chemisorbed. These observations are consistent with previous experimental measurements for the $\text{Al}_{100}^+ + \text{N}_2$ and $\text{Al}_{44}^{+/-} + \text{N}_2$ reactions, and with density functional theory (DFT) studies that were performed to investigate the mechanism of this reaction.^{28,29}

In addition to the reaction cross sections plotted in Figure 2, we also show heat capacities measured for Al_{114}^+ , Al_{115}^+ and Al_{117}^+ plotted against temperature. The heat capacities are taken from Ref. 38. When a macroscopic crystal melts there is a step in the internal energy due to the latent heat. The step in the internal energy leads to a peak in the heat capacity which is delta function for a macroscopic crystal with a melting point. For a cluster, the peak is broadened by finite size effects^{53–55} and liquid-like and solid-like clusters coexist dynamically over a range of temperatures.^{7–9} The center of the peak in the heat capacity is the melting temperature and the area under the peak is the latent heat. For clusters, both the melting temperatures and the latent heats are usually depressed relative to the bulk values primarily because the clusters have a much larger surface to volume ratio than the bulk.⁵⁶ For example, the melting temperatures for the clusters studied here are <700 K while the bulk melting point is 933 K.

As noted above, there are two peaks in the heat capacities for Al_{115}^+ and Al_{117}^+ (and also for Al_{116}^+). There are several possible explanations for the existence of two peaks.³⁹ They could result from different parts of the clusters melting at different temperatures. For example, surface pre-melting is a well-known phenomenon that occurs for some metal surfaces.⁵⁷ The low-temperature peak could result from the melting of the cluster surface with the high-temperature peak resulting from the melting of the core. One argument against this explanation is the large temperature difference (150–200 K) between the two peaks. It is difficult to imagine liquid and solid portions of a cluster coexisting over such a broad temperature range. But even more compelling is the observation that the low temperature peak disappears when the clusters are annealed.³⁹ This indicates that the purported liquid layer does not refreeze, which is difficult to explain because a solid nucleus already exists. Thus the premelting explanation appears to be ruled out.

Another explanation for the two peaks is that one of them is due to a structural transition and the other is due to melting. If the low-temperature peak was due to melting it means that the high-temperature peak must be due to a transition between two liquid structures. A transition between two distinct liquid forms is rare in pure substances and invariably occurs at elevated pressures,^{58–60} so it seems unlikely that the higher temperature peak results from such a process. Thus the most

likely explanation is that the low temperature peak results from a structural transition, and the high temperature peak from melting; in which case the structural transition is between two solid forms. Note that a peak in the heat capacity indicates that the enthalpy increases during the transition and so the solid to solid transition is driven by entropy.

It is evident from Figure 2 that the sharp drop in the kinetic energy thresholds that occur as a function of temperature are correlated with the lower temperature peak in the heat capacities. Furthermore, the kinetic energy thresholds do not change by much in the temperature range associated with the higher temperature peak in the heat capacities (the one attributed to the melting transition).

For Al_{114}^+ there is only a single well-defined peak in the heat capacity (see Figure 2). The higher temperature peak observed for Al_{115}^+ and Al_{117}^+ persists while the lower temperature peak is diminished to the point where its size is comparable to the scatter in the measurements. From the heat capacity measurements alone, it is difficult to say with any degree of certainty whether or not the low temperature peak still exists for Al_{114}^+ . However, there is clearly a sizable drop in the kinetic energy thresholds that is correlated with what appears to be a small peak in the heat capacity at around 450 K.

The drops in the kinetic energy thresholds at around 450 K for all three clusters are around 0.5–0.6 eV. Assuming an Arrhenius relationship for the reaction rates, a decrease in the activation energy of this magnitude corresponds to an increase in the reaction rate constant, $k(T)$ at 450 K, of around 10^6 -fold. In addition to the relatively sharp drop in the thresholds at around 450 K there is a gradual systematic drop in the thresholds as the temperature is raised. The magnitude of the decrease is difficult to define accurately, but it is around $(6 \pm 2) \times 10^{-4}$ eV/K. The internal energy in the 200–1000 K range studied here, calculated using statistical thermodynamics with a frequency distribution derived from a modified Debye model,⁵¹ increases at an average rate of around 2.4×10^{-2} eV/K. If all of the internal energy was available to drive the chemisorption reaction, the kinetic energy threshold would decrease at the same rate as the internal energy increased. But the kinetic energy threshold decreases at a rate which is around 40 times slower than the increase in the internal energy. So at most, only around 2.5% of the increase in the internal energy appears as a decrease in the kinetic energy threshold. Another way to think about this issue is to consider the internal energy to be distributed statistically between the ~ 350 vibrational degrees of freedom in the transition state. In which case, the amount of internal energy in the reaction coordinate should be around 1/350th of the total and so the threshold would be expected to decrease by around 7×10^{-5} eV/K (the rate that the internal energy increases divided by the number of degrees of freedom). A decrease of 7×10^{-5} eV/K is around one tenth of the observed decrease ($(6 \pm 2) \times 10^{-4}$ eV/K). This suggests that something more than a direct effect of the internal energy is responsible for most of the systematic drop in the kinetic energy thresholds that occurs with increasing temperature.

In a recent combined experimental and theoretical study of the chemisorption of N_2 onto $\text{Al}_{44}^{+/-}$, DFT calculations

were used to examine the structure of the intermediates and products, and the collision processes were simulated by DFT molecular dynamics.²⁹ The lowest energy geometries found for $\text{Al}_{44}\text{N}_2^{+/-}$ have the two nitrogen atoms fully reduced by the metal cluster and transformed into separated N^{3-} anions which are located at the surface of the metal cluster. In the global minimum-energy structure one nitrogen atom is embedded in the cluster surface (with four Al–N bonds) and the other is sitting above the surface (with three Al–N bonds). These DFT results are consistent with the *ab initio* calculations of Bai *et al.* which showed that the nitrogen atom in Al_nN clusters prefers a peripheral position for $n > 10$.⁶¹ For smaller clusters, $n \leq 10$, the nitrogen atom prefers to occupy an interior position.^{61–63}

In the density functional molecular dynamics simulations²⁹ a collision geometry with the N_2 axis perpendicular to the cluster surface is unreactive, while a parallel orientation leads to dissociative chemisorption. A barrier height of 3.4 eV was found in the simulations. However, barriers more than 1 eV lower were found in constrained static calculations, indicating a significant dynamic contribution to the measured barrier. The dynamic contribution results because the system has insufficient time to relax to its lowest energy configuration as the collision occurs. The density functional molecular dynamics calculations reproduced the decrease in the activation barrier that is observed in the experiments when the clusters melt. In addition to the sharp drop in the kinetic energy thresholds at the melting transition, a gradual decrease occurs as the temperature is raised. The simulations indicated that both the sharp drop in the kinetic energy thresholds and the gradual decrease were mainly due to an increase in the interatomic distances in the cluster. The gradual decrease is mainly due to the thermal expansion of the cluster, while the sharp decrease in the thresholds at the melting temperature is due to the volume change of melting and to the increase in atomic disorder. According to the simulations, the volume change is the main cause, and the disorder is a minor contributor.

The simulations indicated that both electronic and geometric factors contribute to the lowering of the kinetic energy thresholds.²⁹ Thermal expansion is known to cause the polarizabilities of metal clusters to increase with temperature⁶⁴ implying that the electrons will be more sensitive to external perturbations when the lattice expands. This electronic effect lowers the initial Pauli repulsion and facilitates electron transfer from the aluminum cluster to the approaching N_2 molecule. The separation between the aluminum atoms is also important: once the electron transfer (and ionic-like Al–N bonding) starts, an expanded lattice exerts a larger force along the internuclear axis of N_2 , driving the separation of the two atoms and further reducing the barrier.

The sharp drop in the kinetic energy threshold for Al_{114}^+ , Al_{115}^+ , and Al_{117}^+ that occurs at around 450 K is correlated with the first peak in the heat capacities for Al_{115}^+ and Al_{117}^+ . These peaks have been attributed to structural transitions, and the presence of a peak in the heat capacity indicates that the transition that occurs as the temperature is raised is to a higher enthalpy structure. The entropy change for a reversible process is $\Delta H/T$, and while the structural transition is

not reversible,²⁸ there must still be a substantial increase in the entropy associated with it. This increase in the entropy results from the formation of more disordered structures. However, note that the peak in the heat capacity at around 450 K is much smaller for Al_{114}^+ than for Al_{115}^+ and Al_{117}^+ . It follows that the entropy change associated with the structural transition must be much smaller for Al_{114}^+ than for Al_{115}^+ and Al_{117}^+ , and so it is unlikely that disorder is the main factor responsible for the sharp increase in reactivity at 450 K because the decrease in the kinetic energy threshold is, if anything, larger for Al_{114}^+ than for Al_{115}^+ and Al_{117}^+ . Thus the most likely cause for the decrease in the kinetic energy threshold is an increase in the volume of the cluster due to the structural transition. The structural transition presumably achieves a density equal to that of the liquid so that when the cluster melts there is no significant change in the kinetic energy threshold. This seems to be the most plausible explanation for the results. It is noteworthy that these results imply that a structural transition occurs for Al_{114}^+ without a clear signature in the heat capacity.

Previously we found that the lower temperature peaks in the heat capacities for Al_{115}^+ – Al_{117}^+ can be removed by annealing.³⁹ For annealed clusters, the abrupt changes in the kinetic energy thresholds at around 450 K are expected to disappear and the kinetic energy thresholds below 450 K are expected to be similar to the values above 450 K. However, this has not yet been confirmed experimentally.

CONCLUSIONS

Kinetic energy thresholds have been measured for the chemisorption of N_2 on Al_{114}^+ , Al_{115}^+ , and Al_{117}^+ as a function of cluster temperature. The threshold measurements have been compared to heat capacities determined as a function of temperature. Al_{115}^+ and Al_{117}^+ show two peaks in their heat capacities: a peak at ~ 450 K which is attributed to a structural transition; and a peak at ~ 600 K which is attributed to melting. Al_{114}^+ only shows the peak at around 600 K due to melting. There is a sharp drop in the kinetic energy thresholds for all clusters at around 450 K which is correlated with the position of low temperature peak in the heat capacities for Al_{115}^+ and Al_{117}^+ . These observations differ from our previous studies of smaller clusters ($\text{Al}_{44}^{+/-}$ and Al_{100}^+) where a sharp drop in the kinetic energy threshold for N_2 chemisorption is correlated with the peak in the heat capacity due to melting. In that work, density functional molecular dynamics studies indicated that the sharp drop in the kinetic energy threshold upon melting can be traced mainly to the volume change associated with melting. The increased interatomic spacing lowered the kinetic energy threshold through a combination of electronic and geometric effects. The most plausible explanation for the sharp drop in the kinetic energy thresholds for Al_{114}^+ , Al_{115}^+ , and Al_{117}^+ at ~ 450 K is that the structural transition causes a volume change similar to what occurs in the melting transitions of the smaller clusters. Density functional molecular dynamics simulations are required for the larger clusters studied here to test this explanation.

ACKNOWLEDGMENTS

We gratefully acknowledge the support of the US National Science Foundation under grant 0911462.

- ¹A. Aguado and M. F. Jarrold, *Annu. Rev. Phys. Chem.* **62**, 151 (2011).
- ²M. Schmidt, R. Kusche, W. Kronmüller, B. von Issendorff, and H. Haberland, *Phys. Rev. Lett.* **79**, 99 (1997).
- ³M. Schmidt, R. Kusche, B. von Issendorff, and H. Haberland, *Nature (London)* **393**, 238 (1998).
- ⁴A. A. Shvartsburg and M. F. Jarrold, *Phys. Rev. Lett.* **85**, 2530 (2000).
- ⁵F. Chiro, P. Feiden, S. Zamith, P. Labastie, and J. M. L'Hermite, *J. Chem. Phys.* **129**, 164514 (2008).
- ⁶K. L. Pyfer, J. O. Kafader, A. Yalamanchali, and M. F. Jarrold, *J. Phys. Chem. A* **118**, 4900 (2014).
- ⁷R. S. Berry, J. Jellinek, and G. Natanson, *Chem. Phys. Lett.* **107**, 227 (1984).
- ⁸M. Schmidt, R. Kusche, T. Hippler, J. Donges, W. Kronmüller, B. von Issendorff, and H. Haberland, *Phys. Rev. Lett.* **86**, 1191 (2001).
- ⁹F. Calvo, D. J. Wales, J. P. K. Doye, R. S. Berry, P. Labastie, and M. Schmidt, *Eur. Phys. Lett.* **82**, 43003 (2008).
- ¹⁰S. Chacko, K. Joshi, D. G. Kanhere, and S. A. Blundell, *Phys. Rev. Lett.* **92**, 135506 (2004).
- ¹¹A. Aguado and J. M. López, *Phys. Rev. Lett.* **94**, 233401 (2005).
- ¹²S. Chacko, D. G. Kanhere, and S. A. Blundell, *Phys. Rev. B* **71**, 155407 (2005).
- ¹³E. G. Noya, J. P. K. Doye, D. J. Wales, and A. Aguado, *Eur. Phys. J. D* **43**, 57 (2007).
- ¹⁴S. C. Richtsmeier, E. K. Parks, K. Liu, L. G. Pobo, and S. J. Riley, *J. Chem. Phys.* **82**, 3659 (1985).
- ¹⁵M. E. Geusic, M. D. Morse, S. C. O'Brien, and R. E. Smalley, *Rev. Sci. Instrum.* **56**, 2123 (1985).
- ¹⁶D. J. Trevor, R. L. Whetten, D. M. Cox, and A. Kaldor, *J. Am. Chem. Soc.* **107**, 518 (1985).
- ¹⁷K. M. Creegan and M. F. Jarrold, *J. Am. Chem. Soc.* **112**, 3768 (1990).
- ¹⁸M. F. Jarrold, Y. Ijiri, and U. Ray, *J. Chem. Phys.* **94**, 3607 (1991).
- ¹⁹I. Balteanu, O. P. Balaj, M. K. Beyler, and V. E. Bondybegy, *Int. J. Mass Spectrom.* **255**, 71 (2006).
- ²⁰R. B. Wyrwas, B. L. Yoder, J. T. Maze, and C. C. Jarrold, *J. Phys. Chem. A* **110**, 2157 (2006).
- ²¹R. B. Wyrwas and C. C. Jarrold, *J. Am. Chem. Soc.* **128**, 13688 (2006).
- ²²G. E. Johnson, E. C. Tyo, and A. W. Castleman, *Proc. Natl. Acad. Sci. U.S.A.* **105**, 18108 (2008).
- ²³M. Citir, F. Liu, and P. B. Armentrout, *J. Chem. Phys.* **130**, 054309 (2009).
- ²⁴Y. Xie, F. Dong, S. Heinbuch, J. J. Rocca, and E. R. Bernstein, *Phys. Chem. Chem. Phys.* **12**, 947–959 (2010).
- ²⁵M. P. D'Evelyn and R. J. Madix, *Surf. Sci. Rep.* **3**, 413 (1983).
- ²⁶D. C. Jacobs, *J. Phys: Condens Matter* **7**, 1023 (1995).
- ²⁷M. Okado, *J. Phys: Condens. Matter* **22**, 263003 (2010).
- ²⁸B. Cao, A. K. Starace, O. H. Judd, and M. F. Jarrold, *J. Am. Chem. Soc.* **131**, 2446 (2009).
- ²⁹B. Cao, A. K. Starace, O. H. Judd, I. Bhattacharyya, M. F. Jarrold, J. Lopez, and A. Aguado, *J. Am. Chem. Soc.* **132**, 12906 (2010).
- ³⁰C. M. Neal, A. K. Starace, and M. F. Jarrold, *J. Am. Soc. Mass Spectrom.* **18**, 74 (2007).
- ³¹G. A. Breaux, C. M. Neal, B. Cao, M. F. Jarrold, *Phys. Rev. Lett.* **94**, 173401 (2005).
- ³²C. M. Neal, A. K. Starace, M. F. Jarrold, K. Joshi, S. Krishnamurty, and D. G. Kanhere, *J. Phys. Chem. C* **111**, 17788 (2007).
- ³³C. M. Neal, A. K. Starace, and M. F. Jarrold, *Phys. Rev. B* **76**, 054113 (2007).
- ³⁴M. F. Jarrold, B. Cao, A. K. Starace, C. M. Neal, and O. H. Judd, *J. Chem. Phys.* **129**, 014503 (2008).
- ³⁵A. K. Starace, C. M. Neal, B. Cao, M. F. Jarrold, A. Aguado, and J. M. López, *J. Chem. Phys.* **129**, 144702 (2008).
- ³⁶B. Cao, A. K. Starace, O. H. Judd, and M. F. Jarrold, *J. Chem. Phys.* **130**, 204303 (2009).
- ³⁷A. K. Starace, C. M. Neal, B. Cao, M. F. Jarrold, A. Aguado, and J. M. López, *J. Chem. Phys.* **131**, 044307 (2009).
- ³⁸A. K. Starace, B. Cao, O. H. Judd, I. Bhattacharyya, and M. F. Jarrold, *J. Chem. Phys.* **132**, 034302 (2010).
- ³⁹B. Cao, A. K. Starace, O. H. Judd, I. Bhattacharyya, and M. F. Jarrold, *J. Chem. Phys.* **131**, 124305 (2009).
- ⁴⁰C. M. Neal, G. A. Breaux, B. Cao, A. K. Starace, and M. F. Jarrold, *Rev. Sci. Instrum.* **78**, 075108 (2007).
- ⁴¹B. H. Boo and Z. Liu, *J. Phys. Chem. A* **103**, 1250 (1999).
- ⁴²B. D. Leskiw, A. W. Castleman, C. Ashman, and S. N. Khanna, *J. Chem. Phys.* **114**, 1165 (2001).
- ⁴³P. B. Armentrout, *Int. J. Mass Spectrom.* **200**, 219 (2000).
- ⁴⁴R. D. Levine and R. B. Bernstein, *Molecular Reaction Dynamics* (Oxford University Press, New York, 1974), p. 46.
- ⁴⁵M. E. Weber, J. L. Elkind, and P. B. Armentrout, *J. Chem. Phys.* **84**, 1521 (1986).
- ⁴⁶J. L. Elkind and P. B. Armentrout, *J. Phys. Chem.* **90**, 6576 (1986).
- ⁴⁷F. Liu, R. Liyanage, and P. B. Armentrout, *J. Chem. Phys.* **117**, 132 (2002).
- ⁴⁸L. Tan, F. Liu, and P. B. Armentrout, *J. Chem. Phys.* **124**, 084302 (2006).
- ⁴⁹F. Liu, M. L. Li, L. Tan, and P. B. Armentrout, *J. Chem. Phys.* **128**, 194313 (2008).
- ⁵⁰P. B. Armentrout, L. Parke, C. Hinton, and M. Citir, *ChemPlusChem* **78**, 1157 (2013).
- ⁵¹J. Bohr, "Quantum mode phonon forces between chain molecules," *Int. J. Quantum Chem.* **84**, 249 (2001).
- ⁵²O. K. Rice and H. C. Ramsperger, *J. Am. Chem. Soc.* **50**, 617 (1928).
- ⁵³J. Jellinek, T. L. Beck, and R. S. Berry, *J. Chem. Phys.* **84**, 2783 (1986).
- ⁵⁴R. S. Berry, J. Jellinek, and G. Natanson, *Phys. Rev. A* **30**, 919 (1994).
- ⁵⁵R. S. Berry, *Microscale Thermophys. Eng.* **1**, 1 (1997).
- ⁵⁶P. Pawlow, *Z. Phys. Chem.* **65**, 1 (1909).
- ⁵⁷J. W. M. Franken and J. F. van der Veen, *Phys. Rev. Lett.* **54**, 134 (1985).
- ⁵⁸S. Harrington, R. Zhang, P. H. Poole, F. Sciortino, and H. E. Stanley, *Phys. Rev. Lett.* **78**, 2409 (1997).
- ⁵⁹J. N. Glosli and F. H. Ree, *Phys. Rev. Lett.* **82**, 4659 (1999).
- ⁶⁰Y. Li, J. Li, and F. Wang, *Proc. Nat. Acad. Sci. U.S.A.* **110**, 12209 (2013).
- ⁶¹Q. Bai, B. Song, J. Hou, and P. He, *Phys. Lett. A* **372**, 4545 (2008).
- ⁶²B. B. Averkiev, A. I. Boldyrev, X. Li, and L.-S. Wang, *J. Phys. Chem. A* **111**, 34 (2007).
- ⁶³B. B. Averkiev, S. Call, A. I. Boldyrev, L.-M. Wang, W. Huang, and L.-S. Wang, *J. Phys. Chem. A* **112**, 1873 (2008).
- ⁶⁴S. Kummel, J. Akola, and M. Manninen, *Phys. Rev. Lett.* **84**, 3827 (2000).